

1 **Phenolic metabolites of anthocyanins modulate mechanisms of endothelial function**

2

3 Michael Edwards<sup>1</sup>, Charles Czank<sup>2</sup>, Gary M. Woodward<sup>3</sup>, Aedín Cassidy, Colin D. Kay\*

4 Department of Nutrition, Norwich Medical School, University of East Anglia, Norwich, U.K., NR4

5 7TJ

6

7 \*Corresponding author:

8 Dr Colin D. Kay

9 Faculty of Medicine and Health Sciences (MED 1 Floor 2), Department of Nutrition, Norwich

10 Medical School, University of East Anglia, Norwich, U.K., NR4 7UQ

11 Email: [Colin.Kay@uea.ac.uk](mailto:Colin.Kay@uea.ac.uk); Telephone: +44 (0)1603 591236

12

13

14

15

16

---

<sup>1</sup> Current address: GFA, Ely, Cambridgeshire, CB7 4EX, UK

<sup>2</sup> Current address: Telethon Kids Institute, University of Western Australia, West Perth, Western Australia

<sup>3</sup> Current address: Department of Clinical Biochemistry, Oxford University Hospitals, Oxford

## ABSTRACT

Anthocyanins are reported to have vascular bioactivity, however their mechanisms of action are largely unknown. Evidence suggests that anthocyanins modulate endothelial function, potentially by increasing nitric oxide (NO) synthesis, or enhancing NO bioavailability. This study compared the activity of cyanidin-3-glucoside, its degradation product protocatechuic acid and phase II metabolite, vanillic acid. Production of NO and superoxide, and expression of endothelial NO synthase (eNOS), NADPH oxidase (NOX) and haem oxygenase-1 (HO-1), was established in human vascular cell models. Nitric oxide levels were not modulated by the treatments, although eNOS was upregulated by cyanidin-3-glucoside, and superoxide production was decreased by both phenolic acids. Vanillic acid upregulated p22<sup>phox</sup> mRNA but did not alter NOX protein expression, although trends were observed for p47<sup>phox</sup> downregulation and HO-1 upregulation. Anthocyanin metabolites may therefore modulate vascular reactivity by inducing HO-1 and modulating NOX activity, resulting in reduced superoxide production and improved NO bioavailability.

## KEYWORDS

Endothelium, eNOS, cyanidin, HUVEC, NADPH oxidase

## INTRODUCTION

38

39

40 Epidemiological evidence suggests that higher consumption of anthocyanins, a sub-class of the  
41 flavonoid family of polyphenols <sup>1</sup>, is inversely associated with risk of hypertension <sup>2</sup> and  
42 cardiovascular disease mortality <sup>3,4</sup>. In recent randomised controlled trials, 12-week consumption of  
43 anthocyanins (320 mg/day) was associated with enhanced endothelial function in  
44 hypercholesterolaemic individuals <sup>5</sup>, while acute consumption (724 mg) elicited a dose-dependent  
45 (biphasic) increase in endothelial-dependent vasodilation <sup>6</sup>. Mechanistic studies suggest that  
46 anthocyanins may act to enhance vascular function through modulating levels of nitric oxide (NO) <sup>7</sup>,  
47 <sup>8</sup>. The reduced bioavailability of endothelial-derived NO is critical in the development of  
48 atherosclerosis <sup>9</sup>; and a loss of NO in vascular pathologies is mediated by reaction with superoxide  
49 anion (O<sub>2</sub><sup>-</sup>) <sup>10,11</sup> generated by vascular NADPH oxidase (NOX) enzymes <sup>9,12</sup> which constitute a major  
50 source of reactive oxygen species in the vasculature. Anthocyanins have been reported to elevate the  
51 expression of the cytoprotective enzyme haem oxygenase-1 (HO-1) in human vascular endothelial  
52 cells <sup>13</sup> and upregulation of HO-1 with subsequent inhibition of NOX activity has been described in  
53 cell culture <sup>14</sup> and animal models <sup>15</sup>. Therefore, anthocyanins could potentially improve endothelial  
54 function, by increasing the bioavailability of endothelial-derived NO and thus improving vascular  
55 homeostasis, by decreasing endothelial NOX activity and O<sub>2</sub><sup>-</sup> levels as a result of HO-1 induction.

56

57 Anthocyanins are generally reported to have a low relative bioavailability <sup>16,17</sup>, suggesting their  
58 bioactivity is mediated by their metabolites, which exist in the systemic circulation at much higher  
59 concentrations <sup>17,18</sup> than their precursor structures. However, most previous studies have explored the  
60 activity of anthocyanins *in vitro* as unmetabolised precursor structures, whilst very few have  
61 examined the activity of their phenolic metabolites. The aim of the present study was therefore to  
62 compare the bioactivity of a parent anthocyanin with its physiologically relevant phenolic acid  
63 derivatives, to establish if anthocyanin metabolites share a common or have a differential biological

64 activity to their unmetabolised structures. Cyanidin-3-glucoside (Figure 1A) was chosen for this study  
65 as Czank *et al* (2013) have recently reported the systemic concentrations of its metabolites in humans  
66 using an isotope tracer study design <sup>17, 19</sup>. Of the 24 isotope-labelled metabolites identified, the  
67 phenolic acid degradation product protocatechuic acid (Figure 1B), and its mono-*O*-methylated  
68 metabolite vanillic acid (Figure 1C), were selected for comparison with the parent anthocyanin, as  
69 they share structural similarities with the known vasoactive compound apocynin <sup>2</sup>.

70

71 Bioactivity was assessed by screening physiologically relevant concentrations of the treatments (at  
72 0.1, 1, 10  $\mu\text{M}$  <sup>17</sup>) for effects on eNOS expression and activity, and angiotensin II-stimulated  
73 superoxide production, in human umbilical vein endothelial cells (HUVEC). Vanillic acid was  
74 ultimately selected to explore mechanisms potentially underlying the observed activity, by examining  
75 the modulation of NOX isoforms (and subunits) and HO-1, using both HUVEC and human coronary  
76 artery endothelial cells (HCAEC).

77

## 78 MATERIALS AND METHODS

79

80 **Standards and reagents.** Cyanidin-3-glucoside was purchased from Extrasynthese (Genay Cedex,  
81 France); VAS2870 from Enzo Life Sciences (Exeter, U.K.); and all other reagents were from  
82 Sigma-Aldrich (Poole, U.K.) unless otherwise noted. Stock solutions were prepared in dimethyl  
83 sulphoxide (DMSO) and stored at  $-80^{\circ}\text{C}$ . Foetal bovine serum (FBS, heat-inactivated) was  
84 purchased from Biosera (Ringmer, UK) and tumour necrosis factor-alpha (TNF- $\alpha$ ), TRIzol<sup>®</sup>  
85 reagent, and SuperScript<sup>®</sup> II Reverse Transcriptase were obtained from Life Technologies (Paisley,  
86 UK).

87

88 Precision 2x real-time PCR MasterMix with SYBR<sup>®</sup>Green was obtained from PrimerDesign Ltd  
89 (Southampton, UK). Custom primer sets for human NOX2, NOX4, p22<sup>phox</sup>, p47<sup>phox</sup> and p67<sup>phox</sup>

90 were supplied by PrimerDesign Ltd, and custom primers for human HO-1 (HMOX-1) by Life  
91 Technologies. Primer sequences are provided as Supporting Information (Table S1).

92  
93 NuPAGE sample reducing agent and LDS sample buffer were purchased from Life Technologies,  
94 and Precision Plus Protein Dual Colour standards from Bio-Rad Laboratories, Inc (Hemel  
95 Hempstead, UK).

96  
97 **Cell culture.** Early passage, pooled HUVEC were purchased from TCS Cellworks (Buckingham,  
98 UK) and used between passages 2 to 4. Cells were routinely cultured in large vessel endothelial cell  
99 growth medium (TCS CellWorks) at 37°C and 5% CO<sub>2</sub>. HUVEC were sub-cultured using 0.025%  
100 trypsin and 0.01% ethylenediaminetetraacetic acid (EDTA) (TCS CellWorks).

101  
102 Cryo-preserved, second passage, single donor HCAEC were purchased from PromoCell GmbH  
103 (Heidelberg, Germany) and used between passages 3 to 6. Cells were routinely cultured in  
104 endothelial cell medium MV (PromoCell GmbH) at 37°C and 5% CO<sub>2</sub>. HCAEC were sub-cultured  
105 using 0.04% trypsin and 0.03% EDTA (PromoCell GmbH).

106  
107 **Cytotoxicity assay.** The maximal level of flavonoids and flavonoid metabolites reported in the  
108 systemic circulation is generally below 10 µM<sup>1</sup>, hence this concentration was the maximum *in vitro*  
109 concentration utilised in the present study. Cell viability following exposure to 10 µM of treatment  
110 compounds was determined using cell proliferation reagent WST-1 (Roche Applied Science,  
111 Burgess Hill, U.K.) in accordance with the manufacturer's protocol. The assay was conducted using  
112 fibronectin-coated microplates seeded with HUVECs at a density of ~10,000 cells/well, and  
113 subsequently grown to confluence as determined by light microscopy. After incubation with  
114 treatment compounds for 24 h, 10 µl WST-1 reagent was added to each well, and plates were

115 incubated for a further 4 h. Absorbance was measured at 440 - 450 nm using a microplate reader  
116 [Fluostar/Polarstar Optima, BMG Labtech (Aylesbury, U.K.)].

117

118 **Nitrite/nitrate assay and eNOS enzyme-linked immunosorbent assay (ELISA).** Fibronectin-  
119 coated 24-well plates were seeded with HUVECs at a density of ~30,000 cells/well, and cells grown  
120 to confluence. Cells were then cultured in the absence or presence of treatment compounds (0.1, 1,  
121 or 10  $\mu$ M) for 24 h; after which supernatants were removed and stored at -80°C. Cells were washed  
122 once with warm phosphate-buffered saline (PBS), and then harvested in trypsin/EDTA and trypsin-  
123 blocking solution. Cell suspensions were stored at -80°C until lysis. Nitric oxide production was  
124 assessed using a colourimetric microplate assay (Cayman Chemical Company Nitrate/Nitrite  
125 Colourimetric Assay Kit from Cambridge Bioscience, Cambridge, U.K.) according to the  
126 manufacturer's instructions. The average intra-assay coefficient of variation (CV) was 6.63%  $\pm$   
127 1.10% (mean  $\pm$  SD, n=3) and the inter-assay CV was 2.38% (n=3). Quantification of eNOS in  
128 HUVEC lysates was performed with the Quantikine Human eNOS Immunoassay (R&D Systems,  
129 Abingdon, U.K.) according to the manufacturer's instructions. The average intra-assay CV was  
130 4.67%  $\pm$  1.86% (mean  $\pm$  SD, n=3) and the inter-assay CV was 6.10% (n=3).

131

132 **Stimulated superoxide production assay.** Superoxide production was assessed using a modified  
133 cytochrome c assay<sup>20, 21</sup>. The modified assay utilised fibronectin-coated 24-well plates seeded with  
134 HUVECs at a density of ~50,000 cells/well, and grown to confluence; after which cells were  
135 washed once with warm Medium 199 (supplemented with 2% FBS) and incubated for 16-18 h.  
136 Cells were then washed once with warm PBS, and incubated for 6 h in supplemented phenol-red  
137 free Medium 199 (Invitrogen, Paisley, U.K.) with 0.1  $\mu$ M angiotensin II, 30  $\mu$ M ferricytochrome c,  
138 and 0.1, 1 or 10  $\mu$ M of the treatment compounds or 5  $\mu$ M VAS2870 (selective NOX inhibitor<sup>22</sup>); in  
139 the presence or absence of 65 units superoxide dismutase (SOD). Aliquots of cell supernatants were

140 subsequently transferred to a 96-well microplate for measurement of absorbance at 550 nm. Culture  
141 plates were frozen at -80°C for protein extraction.

142

143 **Direct cytochrome c reduction.** Direct reduction of cytochrome c was assessed by co-incubation  
144 of treatment compounds in cell-free extracts at concentrations of 2, 20, 200 and 2000  $\mu\text{M}$  with 20  
145  $\mu\text{M}$  cytochrome c in PBS at 37 °C, as described previously for catechols and quinols<sup>23</sup>. The  
146 spontaneous reduction of cytochrome c was monitored kinetically at 550 nm over 2 h. Cytochrome  
147 c reduction was quantified using the millimolar extinction coefficient for reduced cytochrome c  
148 ( $29.5 \text{ mM}\cdot\text{cm}^{-1}$ ).

149

150 **Superoxide production.** Cell-free superoxide production by xanthine/xanthine oxidase was  
151 measured using a previously described method<sup>21</sup>. Briefly, 200  $\mu\text{M}$  of cytochrome c, 0.1 U/ml  
152 xanthine oxidase and 200  $\mu\text{M}$  xanthine was added to 1, 10, 100 and 1000  $\mu\text{M}$  of the treatment  
153 compounds in 50 mM sodium phosphate buffer (pH 7.4). The reaction kinetics of cytochrome c was  
154 monitored at 550 nm at 25°C over 15 min (to reaction plateau). Superoxide generated was  
155 determined by subtracting the rate of cytochrome c reduction (increase in absorbance at 550 nm) in  
156 the presence of SOD versus parallel incubations in the absence of SOD.

157

158 **Stimulated NOX isoform/subunit gene expression assay.** Twenty-four well plates (SPL Life  
159 Sciences) coated with fibronectin were seeded with HUVEC at a density of ~30,000 cells/well, and  
160 the cells grown to confluence. Culture medium was then aspirated, and the cells were incubated for  
161 16 - 18 h in M199 supplemented with 2% FBS. Thereafter, the cells were incubated for 4 h in  
162 supplemented M199 alone (basal), or media with 0.1  $\mu\text{M}$  angiotensin II in the presence or absence  
163 of 0.1, 1 or 10  $\mu\text{M}$  vanillic acid. After incubation, the plates were either frozen at -80°C or used for  
164 RNA extraction.

165

166 **Stimulated p47<sup>phox</sup> protein expression assay.** Six-well plates (SPL Life Sciences) coated with  
167 fibronectin were seeded with HUVEC or HCAEC at a density of 100,000 cells/well, and cells were  
168 grown to confluence. Culture medium was then aspirated, and the cells were incubated for 16 - 18 h  
169 in M199 supplemented with 2% FBS (HUVEC only). Cells were subsequently incubated for 5 h in  
170 supplemented M199 alone (basal), or media with 20 ng/ml TNF- $\alpha$  in the presence or absence of 0.1,  
171 1, or 10  $\mu$ M vanillic acid. After incubation, media was aspirated from all wells, and the plates  
172 frozen at -80°C until protein extraction.

173

174 **Endothelial HO-1 expression assay.** Expression of HO-1 mRNA/protein was assessed using  
175 fibronectin-coated 6-well plates (SPL Life Sciences) seeded with HUVEC or HCAEC at a density  
176 of ~100,000 cells/well, and grown to ~70% confluence. Culture medium was then aspirated, and the  
177 cells were incubated for 6 h in supplemented culture medium alone (basal), or media with 10 ng/ml  
178 phorbol 12-myristate 13-acetate (PMA, positive control), vehicle control (0.005% DMSO; HUVEC  
179 only), or 0.1, 1 or 10  $\mu$ M vanillic acid. After incubation, media was aspirated from all wells and the  
180 plates either frozen at -80°C, or used for RNA or protein extraction.

181

182 **Reverse transcription – quantitative polymerase chain reaction.** RNA was extracted from cells  
183 using TRIzol<sup>®</sup> reagent, according to the manufacturer's instructions; and 1  $\mu$ g of each sample  
184 utilised in a reverse transcription reaction with SuperScript<sup>®</sup> II. Analysis of gene expression was  
185 performed using the Applied Biosystems 7500 Real time PCR System (Life Technologies; 7500  
186 software version 2.0) with SYBR<sup>®</sup>Green detection. Typically, 25 ng of cDNA was amplified with  
187 300 nM of the appropriate primer set. Following enzyme activation at 95°C for 10 minutes, 50  
188 cycles of denaturation (15 seconds at 95°C) and data collection (60 seconds at 60°C) were  
189 performed. Relative changes in gene expression were quantified using the comparative C<sub>t</sub> method  
190 <sup>24</sup>. Optimal stably expressed human reference genes for normalisation of C<sub>t</sub> data were identified

191 using a geNormPLUS kit with primer sets for six genes (PPIA, PRDM4, UBE2D2, UBE4A,  
192 TWY1, VIPAS39) supplied by PrimerDesign Ltd.

193

194 **Immunoblot analysis of endothelial NOX isoform/subunit and HO-1 expression.** Cells were  
195 harvested and lysed 1% IGEPAL<sup>®</sup> (octylphenoxy polyethoxyethanol, CA-630), 150 mM NaCl, 20  
196 mM Tris and 10% glycerol (pH 8.0), supplemented with protease inhibitors (Roche Complete  
197 Protease Inhibitor Cocktail). Plates were incubated with lysis buffer for 0.5 h at 4°C, and recovered  
198 solutions subject to cell disruption by oscillation (50 Hz for 5 minutes with Qiagen TissueLyser  
199 LT). After centrifugation at 13,000 rpm (15 minutes at 4°C) the protein content of the supernatants  
200 was assayed using the Pierce BCA Protein Assay Kit (Fisher Scientific U.K. Ltd, Loughborough,  
201 U.K.) according to manufacturer's instructions.

202

203 For SDS-PAGE, cell lysates were reduced using 50 mM dithiothreitol. Briefly, 15 - 25 µg of protein  
204 was loaded onto a 4% polyacrylamide stacking gel, and separated across a 10% resolving gel (at 25  
205 mA for 1 h) prior to semi-dry transfer to Immobilon-FL PVDF membrane (Millipore, Watford, UK)  
206 at 200 mA for 1.5 h. Membranes were blocked for 1 h at room temperature and incubated overnight  
207 (at 4°C) with chicken polyclonal anti-glyceraldehyde-3-phosphate dehydrogenase (GAPDH,  
208 Millipore) or goat polyclonal anti-actin (Santa Cruz Biotechnology, Inc., California, U.S.); and  
209 either rabbit polyclonal anti-gp91phox (Millipore), rabbit polyclonal anti-NOX4 (Abcam,  
210 Cambridge, U.K.), rabbit polyclonal anti-p47<sup>phox</sup> (Santa Cruz Biotechnology, Inc. or Abcam), or  
211 rabbit polyclonal anti-HO-1 (Abcam). Membranes were then washed prior to incubation with either  
212 donkey anti-chicken IgG (IR dye 680 LT) or donkey anti-goat IgG (IR dye 680) and goat anti-rabbit  
213 IgG (IR dye 800 CW) (Li-Cor, Cambridge, U.K.) for 1 h at room temperature. Membranes were  
214 washed and subsequently imaged and quantified using an Odyssey Infrared Imaging System (Li-  
215 Cor; Application Software version 3.0.21).

216

217 **Statistical analysis.** Analysis of variance (ANOVA) with LSD post-hoc test was performed using  
218 SPSS software (IBM, New York, USA) version 18 for Windows. Significance was determined at  
219 the 5% level relative to basal or the assay control. Three biological replicates for each control or  
220 treatment were utilised for analysis unless otherwise noted. Means of biological replicates were  
221 represented graphically, with error bars denoting standard deviation from the mean. For each  
222 control or treatment in the stimulated superoxide production assay, mean absorbance ratio (550  
223 nm/620 nm) in the presence of SOD (n=3) was subtracted from individual absorbance ratio values  
224 in the absence of SOD (n=3), to correct for cytochrome c reduction owing to generated superoxide.  
225 Mean SOD-corrected absorbance ratio for each treatment was then represented graphically as  
226 percentage of that for the angiotensin II control.

227

228

## RESULTS

229

230 **Endothelial cytotoxicity.** All treatments were screened for cytotoxicity at a concentration of 10  
231  $\mu\text{M}$ ; representing the highest concentration used in subsequent bioactivity investigations. No  
232 significant effects ( $p > 0.05$ ) on endothelial cell viability were observed following a 24 h incubation  
233 of HUVECs with 10  $\mu\text{M}$  of any treatment compound (data not shown).

234

235 **Endothelial NO production.** Cyanidin-3-glucoside, and the phenolic derivatives protocatechuic  
236 acid and vanillic acid, did not significantly alter endothelial NO production as measured by levels of  
237 NO decomposition products (nitrite & nitrate) in HUVEC supernatants (Supporting Information,  
238 Figure S1). Resveratrol (100  $\mu\text{M}$ ) and PMA (10 nM) were used as positive controls to confirm the  
239 sensitivity of the assay, and elicited significant increases in total nitrite and nitrate ( $> 270\%$  above  
240 basal levels).

241

242 **eNOS expression in cultured HUVEC.** Significant upregulation of eNOS ( $p < 0.001$ ) was  
243 observed following 24 h incubation of HUVECs with 0.1, 1 & 10  $\mu\text{M}$  cyanidin-3-glucoside (~4 - 7  
244 fold increase; Figure 2A). No significant alteration in eNOS levels was observed at any  
245 concentration of protocatechuic acid (Figure 2B) or vanillic acid (Figure 2C).

246  
247 **Stimulated endothelial superoxide production.** The generation of superoxide anion was  
248 confirmed using a previously reported NOX inhibitor VAS2870<sup>22</sup>, in the presence and absence of  
249 angiotensin II, where co-incubation with VAS2870 significantly reduced superoxide production ( $p$   
250  $< 0.01$ ) (Supporting Information, Figure S2).

251  
252 Significantly elevated superoxide levels were detected following incubation of cells with 0.1  $\mu\text{M}$   
253 and 1  $\mu\text{M}$  cyanidin-3-glucoside (~3 fold increase; Figure 3A), relative to the angiotensin II-  
254 stimulated control. A significant decrease in superoxide ( $p < 0.001$ ) was induced by protocatechuic  
255 acid, at 10  $\mu\text{M}$  (~5 fold decrease; Figure 3B), whilst vanillic acid elicited statistically significant  
256 reductions ( $p < 0.05$ ) in superoxide at all concentrations examined (~2 fold decrease at 1  $\mu\text{M}$ ;  
257 Figure 3C). A linear dose-response relationship was not evident for any treatment. Control  
258 experiments were conducted to exclude possible confounding through direct reduction of  
259 cytochrome c, or scavenging of NOX-derived superoxide radicals, by the treatments. There was no  
260 significant impact on cytochrome c reduction ( $\leq 0.02 \text{ nmole.h}^{-1}$ ) or superoxide levels (75-106% of  
261 control) during incubations with treatment compounds at concentrations up to 10  $\mu\text{M}$  in cell-free  
262 systems.

263  
264 **Stimulated endothelial gene expression of NOX isoforms and subunits.** Vanillic acid was  
265 examined for effects on stimulated endothelial gene expression of the NOX2 and NOX4 isoforms,  
266 and the associated subunits p22<sup>phox</sup>, p47<sup>phox</sup>, and p67<sup>phox</sup>. Real time PCR melt curve data indicated  
267 non-specific amplification for NOX2, p47<sup>phox</sup>, and p67<sup>phox</sup> primer sets (data not shown); therefore

268 relative quantification of gene expression was performed for NOX4 and p22<sup>phox</sup> only. Co-incubation  
269 of HUVEC with angiotensin II and vanillic acid (0.1, 1 and 10  $\mu$ M) for four hours elicited no  
270 significant differences in NOX4 mRNA compared to the angiotensin II control ( $p > 0.05$ ; Figure  
271 4A). A statistically significant ( $p < 0.05$ ) upregulation of p22<sup>phox</sup> mRNA levels was observed with  
272 vanillic acid at 0.1  $\mu$ M and 1  $\mu$ M (Figure 4B).

273

274 **Stimulated endothelial protein expression of NOX isoforms and subunits.** The modulation of  
275 NOX2 and NOX4 isoforms by vanillic acid was further characterised at the protein level. Following  
276 angiotensin II stimulation, weak immunoreactive bands corresponding to NOX2 were visualised by  
277 immunoblotting of endothelial lysates, such that quantification of bands by densitometry was not  
278 possible (data not shown). By contrast, angiotensin II-induced upregulation of NOX4 expression  
279 was observed, although this was not significantly modulated ( $p > 0.05$ ) by co-incubation of cells  
280 with angiotensin II and vanillic acid at any concentration examined (0.1-10  $\mu$ M) (Figure 5).

281

282 The effect of vanillic acid on stimulated protein expression of the key NOX2 subunit p47<sup>phox</sup> was  
283 also investigated as a possible mechanism of NOX inhibition. Following co-incubation of HUVEC  
284 with 20 ng/ml TNF- $\alpha$  and increasing concentrations of vanillic acid (0.1, 1, or 10  $\mu$ M) for five  
285 hours, a trend towards decreased p47<sup>phox</sup> expression was observed relative to TNF- $\alpha$  alone (Figure  
286 6A), although these changes were not statistically significant ( $p = 0.06$  at 1  $\mu$ M and 10  $\mu$ M vanillic  
287 acid). A confirmatory experiment was conducted using the HCAEC model, but here no effect was  
288 detected on TNF- $\alpha$  stimulated p47<sup>phox</sup> expression ( $p > 0.05$ ; Figure 6B).

289

290 **Endothelial HO-1 expression.** Modulation of HO-1 expression by vanillic acid was examined as a  
291 putative indirect mechanism of NOX inhibition. Incubation of HUVEC with the protein kinase C  
292 activator PMA (at 10 ng/ml) for six hours induced a significant increase in basal HO-1 mRNA  
293 levels ( $p < 0.001$  versus vehicle control; Figure 7). Vanillic acid, at concentrations of 0.1, 1 and 10

294  $\mu\text{M}$ , elicited a concentration-dependent elevation in endothelial HO-1 mRNA ( $\sim 1.6$ -fold versus  
295 unstimulated cells with  $10 \mu\text{M}$  vanillic acid), with a trend towards significance compared to vehicle  
296 control ( $p = 0.1$ ) at  $10 \mu\text{M}$  (Figure 7). Trends towards elevated expression of HO-1 protein in  
297 HUVEC were also observed following a six hour incubation with PMA ( $\sim 1.9$ -fold increase versus  
298 unstimulated cells) or vanillic acid ( $\sim 1.8$ -fold increase at  $1 \mu\text{M}$  vanillic acid) relative to the vehicle  
299 control ( $p = 0.07$  and  $p = 0.1$  respectively; Figure 8A). Since the vehicle control (0.005% DMSO)  
300 also appeared to upregulate HO-1 protein, vanillic acid was prepared directly in aqueous solution  
301 for use in the HCAEC model, to exclude any vehicle-related effects. Expression of HO-1 protein  
302 was slightly elevated following a 6 hour incubation with PMA in the HCAEC model ( $\sim 1.2$ -fold  
303 increase versus unstimulated cells; Figure 8B). An apparent upregulation of HO-1 protein was  
304 observed at all concentrations of vanillic acid tested (Figure 8B), with a trend towards significance  
305 at  $1 \mu\text{M}$  ( $\sim 1.8$ -fold increase;  $p = 0.07$ ) relative to basal.

306

307

## DISCUSSION

308

309 The low bioavailability of parent anthocyanins suggests their bioactivity *in vivo* is mediated by  
310 phenolic metabolites, which have recently been reported as the main circulating species following  
311 anthocyanin consumption<sup>17-19</sup>. Here, we report that phenolic metabolites appear to modulate  
312 vascular endothelial cell function through alternative mechanisms to those previously described for  
313 parent anthocyanins. In the present study, the parent anthocyanin increased eNOS expression,  
314 whereas phenolic derivatives had no effect. However, these metabolites elicited reductions in  
315 superoxide production, which could subsequently decrease scavenging of NO. Recent studies by  
316 Czank *et al* (2013) and de Ferrars *et al* (2014) have confirmed a physiologically appropriate range  
317 for anthocyanin metabolites in humans of  $0.1 - 10 \mu\text{M}$ <sup>17-19</sup> and the present study assessed potential  
318 mechanisms of activity at these concentrations. Indeed, following consumption of  $500 \text{ mg } ^{13}\text{C}$ -  
319 labelled cyanidin-3-glucoside, a serum  $C_{\text{max}}$  of  $1.85 \mu\text{M}$  has been reported for vanillic acid, with 1

320  $\mu\text{M}$  concentrations persisting for up to 24 hours<sup>19</sup>; suggesting phenolic derivatives of anthocyanins  
321 may be present in the systemic circulation at low micromolar levels for at least 18-24 hours after  
322 ingestion of parent anthocyanins. Based on our findings, physiologically relevant levels of  
323 anthocyanin metabolites are likely to act indirectly to maintain vascular homeostasis, through  
324 induction of HO-1 and decreased endothelial superoxide generation, as opposed to directly  
325 stimulating eNOS activity and NO production.

326  
327 Endothelium-derived nitric oxide is a key component of vascular homeostasis<sup>11</sup> and prior *in vitro*  
328 studies have described both upregulation and activation of the eNOS enzyme by anthocyanins  
329 (including cyanidin-3-glucoside) in cultured endothelial cells at concentrations ranging from 0.001  
330  $\mu\text{M}$  up to 250  $\mu\text{M}$ <sup>7, 8, 13</sup>. Interestingly, in the present study we observed differential bioactivity for  
331 cyanidin-3-glucoside relative to its phenolic acid derivatives. Specifically, no treatment compounds  
332 significantly modulated endothelial NO production, however, cyanidin-3-glucoside significantly  
333 upregulated eNOS protein levels, while the phenolic derivatives remained inactive (Figure 2).

334  
335 NOX enzymes represent a major source of reactive oxygen species in the vasculature<sup>12, 25</sup> and  
336 anthocyanin metabolites could act as endothelial NOX inhibitors, based on previously reported  
337 structure-activity studies<sup>21</sup>. In the current study, differential bioactivity was again observed for  
338 cyanidin-3-glucoside relative to its phenolic acid derivatives. A significant elevation in superoxide  
339 levels was elicited by cyanidin-3-glucoside; and in contrast, both protocatechuic acid and vanillic  
340 acid significantly reduced superoxide levels (Figure 3). Whilst previous reports have described  
341 superoxide scavenging<sup>26</sup> and direct cytochrome c reduction<sup>27</sup> elicited by flavonoids, such activity  
342 is reported at much higher concentrations (~40 - 100  $\mu\text{M}$ ) than those used in the current  
343 investigation ( $\leq 10\mu\text{M}$ ), and control experiments in cell-free incubations confirmed negligible  
344 superoxide scavenging or direct cytochrome c reduction by the treatments. High concentrations of  
345 phenolic compounds in culture medium have also been reported to result in the generation of

346 hydrogen peroxide <sup>28</sup>, which could potentially interfere with assay methodologies; however, only  
347 minimal hydrogen peroxide formation has previously been reported for delphinidin (at 10  $\mu\text{M}$ ) <sup>28</sup>  
348 which is one of the most reactive anthocyanins <sup>29</sup>. Therefore, data from cell-free experiments in the  
349 current study indicate that the treatment compounds do not directly scavenge superoxide radicals, as  
350 negligible activity was observed, and the present findings likely reflect reduced endothelial  
351 superoxide generation as opposed to radical scavenging.

352

353 The phenolic derivative vanillic acid (the methylated metabolite of protocatechuic acid) was  
354 subsequently selected to explore mechanisms potentially underlying the observed reductions in  
355 superoxide production. In the present study, vanillic acid at a concentration of 1  $\mu\text{M}$  significantly  
356 reduced endothelial superoxide levels, which is comparable to the  $C_{\text{max}}$  value reported by Czank *et*  
357 *al* (2013) for <sup>13</sup>C-labelled phase II conjugates of protocatechuic acid (2.35  $\mu\text{M}$ ) following ingestion  
358 of <sup>13</sup>C-labelled cyanidin-3-glucoside <sup>17</sup>. Steffen *et al* (2008) have previously described NOX  
359 inhibitory activity of vanillic acid in disintegrated HUVEC ( $\text{IC}_{50} = 8.1 \mu\text{M}$ ), with minimal direct  
360 superoxide scavenging activity in a cell-free system ( $\text{IC}_{50} > 100 \mu\text{M}$ ) <sup>21</sup>; which was confirmed by  
361 the absence of direct superoxide scavenging by vanillic acid in the present study.

362

363 NOX4 is reported to be the major vascular endothelial isoform <sup>30, 31</sup>, producing mainly hydrogen  
364 peroxide <sup>32</sup>; and whilst NOX4-derived hydrogen peroxide would not act to limit NO bioavailability  
365 <sup>33</sup>, it might induce vasodilation through hyperpolarisation independently of NO activity <sup>34</sup>. In  
366 contrast NOX2 generates superoxide <sup>35</sup> and may have a key role in regulating vascular function <sup>32</sup>,  
367 <sup>36</sup>. Both NOX2 and NOX4 associate with the integral membrane protein p22<sup>phox</sup> <sup>37</sup>, but activation of  
368 NOX2 follows the recruitment of additional cytosolic proteins including p47<sup>phox</sup> ('organiser'  
369 subunit) and p67<sup>phox</sup> ('activator' subunit) <sup>37, 38</sup>. Modulation of the expression of NOX2 and NOX4  
370 isoforms, and associated subunits (p22<sup>phox</sup>, p47<sup>phox</sup>, and p67<sup>phox</sup>) by vanillic acid was therefore  
371 explored using RT-qPCR. Co-incubation of angiotensin II with vanillic acid elicited no significant

372 changes in levels of endothelial NOX4 mRNA relative to angiotensin II alone (Figure 4A).  
373 However, a significant upregulation of p22<sup>phox</sup> mRNA levels was observed with 0.1 and 1  $\mu$ M  
374 vanillic acid (Figure 4B), whilst we were unable to assess transcriptional modulation of the  
375 superoxide-generating NOX2 isoform, or p47<sup>phox</sup> and p67<sup>phox</sup>. Therefore the effects of vanillic acid  
376 on the stimulated expression of NOX2 and p47<sup>phox</sup>, and also NOX4, were explored at the protein  
377 level.

378

379 There was no significant modulation of stimulated NOX4 protein expression by vanillic acid  
380 (Figure 5), indicating that this particular metabolite does not affect endothelial NOX4 protein.  
381 NOX2 expression was more difficult to discern by immunoblotting of cell lysates, which may  
382 reflect low mRNA/protein expression in vascular cells, and/or poor antibody specificity; although  
383 upregulation of NOX2 in HUVECs following angiotensin II stimulation has been previously  
384 reported <sup>20</sup>. Interestingly, the observed elevation in p22<sup>phox</sup> mRNA induced by vanillic acid did not  
385 appear to be associated with increased NOX4 or NOX2 protein levels. Modulation of p47<sup>phox</sup>  
386 protein expression was examined as a possible mechanism of NOX2 inhibition, and here a trend  
387 was observed towards downregulation of p47<sup>phox</sup> protein following co-incubation with TNF- $\alpha$  and  
388 vanillic acid (Figure 6A). Interestingly, in the HCAEC model, vanillic acid did not modulate  
389 stimulated p47<sup>phox</sup> expression (Figure 6B), and thus vanillic acid does not appear to significantly  
390 alter p47<sup>phox</sup> levels (under the present conditions) and therefore affect NOX2 activity by this  
391 mechanism. However, the anthocyanidin delphinidin has recently been reported to inhibit p47<sup>phox</sup>  
392 translocation and NOX activity in human dermal fibroblasts <sup>39</sup>, suggesting another potential  
393 mechanism by which anthocyanins and/or their degradation products could modulate NOX  
394 function.

395

396 Upregulation of HO-1 has been reported to inhibit NOX function <sup>14, 15</sup>; and previous studies have  
397 described induction of HO-1 expression by anthocyanins and/or their metabolites in human

398 endothelial cells<sup>13, 40</sup>. For example, Nrf2 nuclear translocation and HO-1 expression in cultured  
399 HUVEC was elicited by serum samples obtained from healthy subjects following ingestion of 160  
400 mg purified anthocyanins, which may reflect activity of anthocyanin metabolites as opposed to  
401 parent compounds<sup>40</sup>. Moreover, delphinidin-3-glucoside has previously been reported to enhance  
402 survival of murine hepatocytes exposed to a cytotoxic concentration of epigallocatechin-3-gallate  
403 through upregulation of HO-1 mRNA levels<sup>41</sup>. Endothelial homeostasis is maintained through the  
404 action of vasodilators such as NO, however NO bioactivity is diminished by radicals such as O<sub>2</sub><sup>-</sup>  
405 which are produced through activation of NOX<sup>9, 12</sup>. Anthocyanin metabolites could potentially  
406 indirectly maintain vascular homeostasis by inducing HO-1, with subsequent inhibition of NOX  
407 activity, thus reducing the scavenging of NO by NOX-derived superoxide<sup>14, 15, 40</sup>. Therefore the  
408 potential indirect effect of vanillic acid on NOX activity was explored by assessing modulation of  
409 endothelial HO-1 expression. Following exposure of HUVEC to vanillic acid, elevated HO-1  
410 mRNA levels were observed in what appeared to be a concentration-dependent response (Figure 7),  
411 with a trend towards significance relative to the vehicle control (at 10 μM vanillic acid). Likewise,  
412 vanillic acid increased HUVEC HO-1 protein expression (Figure 8A), and densitometric analysis  
413 indicated a trend towards significance at 1 μM. The vehicle control also appeared to moderately  
414 upregulate HO-1, reflecting previously reported studies in HUVEC with low concentrations of  
415 DMSO (0 - 0.8%)<sup>42</sup>. As such, vanillic acid was prepared directly in aqueous solution for  
416 investigation in the HCAEC model; where a similar trend for upregulation of HO-1 protein was  
417 evident (at 1 μM; Figure 8B), suggesting an inverted U-shaped dose-response.

418

419 A possible limitation of the current investigation was the use of HUVEC as an *in vitro* model.  
420 Whilst HUVEC are widely used for research concerning general properties of endothelial cells<sup>43</sup>,  
421 an arterial endothelial cell type may be more appropriate for studies investigating the potential  
422 modulation of NOX activity in relation to endothelial dysfunction. Thus as part of the current  
423 investigation confirmatory studies were conducted for potential modulation of p47<sup>phox</sup>/HO-1

424 expression, using HCAEC as a more physiologically representative endothelial model. Furthermore,  
425 in the present study there was no effect of cyanidin-3-glucoside on endothelial NO production  
426 (Supporting Information, Figure S1), despite a previous report of activation of eNOS by cyanidin-3-  
427 glucoside at concentrations of  $\leq 5 \mu\text{M}$  in HUVECs <sup>7</sup>. It is possible that assessing eNOS activity by  
428 investigating enzyme phosphorylation, as described previously for blackcurrant anthocyanins in a  
429 HUVEC model <sup>44</sup>, could have provided further information as to the effects of treatment  
430 compounds upon eNOS. NO production was clearly increased by PMA and resveratrol in control  
431 experiments, indicating adequate assay sensitivity for the detection of NO-derived nitrite/nitrate in  
432 aqueous solution. It is however possible that the assay was not sensitive enough to detect subtle  
433 changes in nitrite/nitrate. Interestingly, and with the possible exception of the upregulation of eNOS  
434 by cyanidin-3-glucoside, linear dose-response relationships were not observed for any treatment in  
435 the current investigation, suggesting differential bioactivity of anthocyanins and their metabolites  
436 across dose ranges, as described previously for cyanidin-3-glucoside <sup>8</sup>. However, as only three  
437 concentrations of the treatment compounds were assessed in the current study, it is not possible to  
438 draw definitive conclusions regarding dose-response relationships, and a wider dosage range is  
439 required to confirm our observations.

440

441 Another limitation of the present study was the poor qPCR specificity observed for NOX2, p47<sup>phox</sup>  
442 and p67<sup>phox</sup>, which precluded determination of relative changes in expression for these transcripts.  
443 Previously reported studies have suggested low or no endothelial expression of NOX2 mRNA <sup>30, 45</sup>,  
444 and low expression of p47<sup>phox</sup> and p67<sup>phox</sup> mRNA in HUVEC <sup>30</sup>. Moreover, minimal changes were  
445 detected in NOX4 gene expression, and p47<sup>phox</sup> protein expression, following stimulation with  
446 angiotensin II or TNF- $\alpha$  respectively; although limited upregulation of p47<sup>phox</sup> was consistent in  
447 both HUVEC and HCAEC models.

448

449 In the present study, cyanidin-3-glucoside significantly upregulated endothelial expression of eNOS  
450 as previously reported for unmetabolised anthocyanins<sup>8, 13</sup>, however the phenolic acid derivatives  
451 were not active. By contrast, both the degradation product protocatechuic acid, and its phase II  
452 metabolite vanillic acid, significantly reduced endothelial superoxide levels; whereas the parent  
453 anthocyanin did not. These data suggest a differential bioactivity of anthocyanins relative to their  
454 phenolic derivatives. Our findings therefore indicate that anthocyanins may directly stimulate  
455 eNOS, eliciting improved endothelial function; however, when anthocyanins are metabolized, this  
456 direct effect upon eNOS is lost. Nevertheless, their metabolites could maintain vascular homeostasis  
457 through indirectly preserving NO bioactivity, by mechanisms involving NOX or HO-1. It must be  
458 noted that Czank *et al* (2013) identified 16 phenolic metabolites of cyanidin-3-glucoside in human  
459 serum<sup>17</sup>, which should all be investigated for potential vascular bioactivity in future studies.  
460 Indeed, preliminary data from ongoing studies in our laboratory suggest PCA, and PCA in  
461 combination with VA, upregulate HO-1 protein expression in rat aortic smooth muscle cells *in vitro*  
462 (data not shown).

463

464 In conclusion, there was no direct effect of vanillic acid on endothelial protein expression of eNOS  
465 or NOX isoforms in the present investigation, whereas HO-1 protein was modestly increased;  
466 indicating different mechanisms of bioactivity for phenolic derivatives relative to parent  
467 anthocyanins. This also suggests a potential indirect activity of anthocyanin metabolites in  
468 maintaining vascular homeostasis *in vivo*.

469

## ABBREVIATIONS USED

470  
471  
472 Ang II, angiotensin II; ANOVA, analysis of variance; CV, coefficient of variation; DMSO,  
473 dimethyl sulphoxide; EDTA, ethylenediaminetetraacetic acid; ELISA, enzyme-linked  
474 immunosorbent assay; eNOS, endothelial nitric oxide synthase; FBS; foetal bovine serum; GAPDH,  
475 glyceraldehyde-3-phosphate dehydrogenase; HCAEC, human coronary artery endothelial cell; HO-  
476 1, haem oxygenase-1; HUVEC, human umbilical vein endothelial cell; NADPH, reduced  
477 nicotinamide adenine dinucleotide phosphate; NO, nitric oxide; NOX, NADPH oxidase; O<sub>2</sub><sup>-</sup>,  
478 superoxide; PBS, phosphate-buffered saline; PMA, phorbol 12-myristate 13-acetate; SOD,  
479 superoxide dismutase; TNF- $\alpha$ , tumour necrosis factor-alpha; VA, vanillic acid.

## ACKNOWLEDGEMENTS

481  
482  
483 This study was supported by a two **UK Biotechnology and Biological Sciences Research Council**  
484 **(BBSRC) CASE studentships (M. Edwards & Gary Woodward) in partnership with**  
485 **GlaxoSmithKline (UK). The authors would like to thank Ilde Rodriguez-Ramiro and Emily Warner**  
486 **(Department of Nutrition, Norwich Medical School, University of East Anglia) for their work on**  
487 **the bioactivity of flavonoids and phenolic metabolites in rat aortic smooth muscle cells (supported**  
488 **by the BBSRC Diet and Health Research Industry Club; BB/H004963/1, BB/I006028/1).**

489 The authors have declared no conflict of interest.

## SUPPORTING INFORMATION DESCRIPTION

491  
492  
493 Primer sequences for custom primer sets (human HMOX-1, NOX2, NOX4, p22<sup>phox</sup>, p47<sup>phox</sup> and  
494 p67<sup>phox</sup>) are provided as Supporting Information.

495

496

## REFERENCES

497

498 1. Crozier A., Jaganath I. B.; Clifford M. N. Dietary phenolics: chemistry, bioavailability and  
499 effects on health. *Nat. Prod. Rep.* **2009**, *26*, 1001-43.

500 2. Cassidy A., O'Reilly E. J., Kay C., Sampson L., Franz M., Forman J., Curhan G.; Rimm E. B.  
501 Habitual intake of flavonoid subclasses and incident hypertension in adults. *Am. J Clin. Nutr.* **2010**,  
502 *93*, 338-47.

503 3. Mink P. J., Scrafford C. G., Barraj L. M., Harnack L., Hong C. P., Nettleton J. A.; Jacobs D. R.,  
504 Jr. Flavonoid intake and cardiovascular disease mortality: a prospective study in postmenopausal  
505 women. *Am. J Clin. Nutr.* **2007**, *85*, 895-909.

506 4. McCullough M. L., Peterson J. J., Patel R., Jacques P. F., Shah R.; Dwyer J. T. Flavonoid intake  
507 and cardiovascular disease mortality in a prospective cohort of US adults. *Am. J Clin. Nutr.* **2012**,  
508 *95*, 454-64.

509 5. Zhu Y., Xia M., Yang Y., Liu F., Li Z., Hao Y., Mi M., Jin T.; Ling W. Purified Anthocyanin  
510 Supplementation Improves Endothelial Function via NO-cGMP Activation in Hypercholesterolemic  
511 Individuals. *Clin. Chem.* **2011**, *57*, 1524-33.

512 6. Rodriguez-Mateos A., Rendeiro C., Bergillos-Meca T., Tabatabaee S., George T. W., Heiss C.;  
513 Spencer J. P. Intake and time dependence of blueberry flavonoid-induced improvements in vascular  
514 function: a randomized, controlled, double-blind, crossover intervention study with mechanistic  
515 insights into biological activity. *Am. J Clin. Nutr.* **2013**, *98*, 1179-91.

516 7. Xu J. W., Ikeda K.; Yamori Y. Cyanidin-3-glucoside regulates phosphorylation of endothelial  
517 nitric oxide synthase. *FEBS Lett.* **2004**, *574*, 176-80.

518 8. Xu J. W., Ikeda K.; Yamori Y. Upregulation of endothelial nitric oxide synthase by cyanidin-3-  
519 glucoside, a typical anthocyanin pigment. *Hypertension.* **2004**, *44*, 217-22.

520 9. Higashi Y., Noma K., Yoshizumi M.; Kihara Y. Endothelial function and oxidative stress in  
521 cardiovascular diseases. *Circ. J.* **2009**, *73*, 411-8.

- 522 10. Wever R., Stroes E.; Rabelink T. J. Nitric oxide and hypercholesterolemia: a matter of oxidation  
523 and reduction? *Atherosclerosis*. **1998**, *137 Suppl*, S51-60.
- 524 11. Naseem K. M. The role of nitric oxide in cardiovascular diseases. *Mol. Aspects Med.* **2005**, *26*,  
525 33-65.
- 526 12. Bonomini F., Tengattini S., Fabiano A., Bianchi R.; Rezzani R. Atherosclerosis and oxidative  
527 stress. *Histol. Histopathol.* **2008**, *23*, 381-90.
- 528 13. Sorrenti V., Mazza F., Campisi A., Di Giacomo C., Acquaviva R., Vanella L.; Galvano F. Heme  
529 oxygenase induction by cyanidin-3-O-beta-glucoside in cultured human endothelial cells. *Mol.*  
530 *Nutr. Food Res.* **2007**, *51*, 580-6.
- 531 14. Jiang F., Roberts S. J., Datla S.; Dusting G. J. NO modulates NADPH oxidase function via  
532 heme oxygenase-1 in human endothelial cells. *Hypertension.* **2006**, *48*, 950-7.
- 533 15. Datla S. R., Dusting G. J., Mori T. A., Taylor C. J., Croft K. D.; Jiang F. Induction of Heme  
534 Oxygenase-1 In Vivo Suppresses NADPH Oxidase–Derived Oxidative Stress. *Hypertension.* **2007**,  
535 *50*, 636-42.
- 536 16. Vitaglione P., Donnarumma G., Napolitano A., Galvano F., Gallo A., Scalfi L.; Fogliano V.  
537 Protocatechuic acid is the major human metabolite of cyanidin-glucosides. *J Nutr.* **2007**, *137*, 2043-  
538 8.
- 539 17. Czank C., Cassidy A., Zhang Q., Morrison D. J., Preston T., Kroon P. A., Botting N. P.; Kay C.  
540 D. Human metabolism and elimination of the anthocyanin, cyanidin-3-glucoside: a <sup>13</sup>C-tracer study.  
541 *Am. J Clin. Nutr.* **2013**, *97*, 995-1003.
- 542 18. de Ferrars R. M., Cassidy A., Curtis P.; Kay C. D. Phenolic metabolites of anthocyanins  
543 following a dietary intervention study in post-menopausal women. *Mol. Nutr. Food Res.* **2014**, *58*,  
544 490-502.
- 545 19. de Ferrars R. M., Czank C., Zhang Q., Botting N. P., Kroon P. A., Cassidy A.; Kay C. D. The  
546 pharmacokinetics of anthocyanins and their metabolites in humans. *Br. J Pharmacol.* **2014**, *171*,  
547 3268-82.

- 548 20. Rueckschloss U., Quinn M. T., Holtz J.; Morawietz H. Dose-dependent regulation of NAD(P)H  
549 oxidase expression by angiotensin II in human endothelial cells: protective effect of angiotensin II  
550 type 1 receptor blockade in patients with coronary artery disease. *Arterioscler. Thromb. Vasc. Biol.*  
551 **2002**, 22, 1845-51.
- 552 21. Steffen Y., Gruber C., Schewe T.; Sies H. Mono-O-methylated flavanols and other flavonoids  
553 as inhibitors of endothelial NADPH oxidase. *Arch. Biochem. Biophys.* **2008**, 469, 209-19.
- 554 22. Stielow C., Catar R. A., Muller G., Wingler K., Scheurer P., Schmidt H. H.; Morawietz H.  
555 Novel Nox inhibitor of oxLDL-induced reactive oxygen species formation in human endothelial  
556 cells. *Biochem. Biophys. Res. Commun.* **2006**, 344, 200-5.
- 557 23. Saleem M. M.; Wilson M. T. Kinetic studies on the reduction of cytochrome c. Reaction with  
558 dihydroxy conjugated compounds (catechols and quinols). *Biochem J.* **1982**, 201, 433-44.
- 559 24. Schmittgen T. D.; Livak K. J. Analyzing real-time PCR data by the comparative C(T) method.  
560 *Nat. Protoc.* **2008**, 3, 1101-8.
- 561 25. Bedard K.; Krause K. H. The NOX family of ROS-generating NADPH oxidases: physiology  
562 and pathophysiology. *Physiol. Rev.* **2007**, 87, 245-313.
- 563 26. Taubert D., Breitenbach T., Lazar A., Censarek P., Harlfinger S., Berkels R., Klaus W.; Roesen  
564 R. Reaction rate constants of superoxide scavenging by plant antioxidants. *Free Rad. Biol. Med.*  
565 **2003**, 35, 1599-607.
- 566 27. Skemiene K., Rakauskaite G., Trumbeckaite S., Liobikas J., Brown G. C.; Borutaite V.  
567 Anthocyanins block ischaemia-induced apoptosis in the perfused heart and support mitochondrial  
568 respiration potentially by reducing cytosolic cytochrome c. *Int. J Biochem. Cell. Biol.* **2012**, 45, 23-  
569 9.
- 570 28. Long L. H., Hoi A.; Halliwell B. Instability of, and generation of hydrogen peroxide by,  
571 phenolic compounds in cell culture media. *Arch. Biochem. Biophys.* **2010**, 501, 162-9.
- 572 29. Woodward G., Kroon P., Cassidy A.; Kay C. Anthocyanin stability and recovery: implications  
573 for the analysis of clinical and experimental samples. *J Agric. Food Chem.* **2009**, 57, 5271-8.

- 574 30. Ago T., Kitazono T., Ooboshi H., Iyama T., Han Y. H., Takada J., Wakisaka M., Ibayashi S.,  
575 Utsumi H.; Iida M. Nox4 as the Major Catalytic Component of an Endothelial NAD(P)H Oxidase.  
576 *Circulation*. **2004**, *109*, 227-33.
- 577 31. Takac I., Schroder K.; Brandes R. P. The Nox Family of NADPH Oxidases: Friend or Foe of  
578 the Vascular System? *Curr. Hypertens. Rep.* **2011**, *14*, 70-8.
- 579 32. Brown D. I.; Griendling K. K. Nox proteins in signal transduction. *Free Radic. Biol. Med.* **2009**,  
580 *47*, 1239-53.
- 581 33. Brandes R. P., Takac I.; Schroder K. No Superoxide--No Stress?: Nox4, the Good NADPH  
582 Oxidase! *Arterioscler. Thromb. Vasc. Biol.* **2011**, *31*, 1255-7.
- 583 34. Ray R., Murdoch C. E., Wang M., Santos C. X., Zhang M., Alom-Ruiz S., Anilkumar N.,  
584 Ouattara A., Cave A. C., Walker S. J., Grieve D. J., Charles R. L., Eaton P., Brewer A. C.; Shah A.  
585 M. Endothelial Nox4 NADPH Oxidase Enhances Vasodilatation and Reduces Blood Pressure In  
586 Vivo. *Arterioscler. Thromb. Vasc. Biol.* **2011**, *31*, 1368-76.
- 587 35. Brandes R. P., Weissmann N.; Schroder K. NADPH oxidases in cardiovascular disease. *Free*  
588 *Radic. Biol. Med.* **2010**, *49*, 687-706.
- 589 36. Schroder K. Isoform specific functions of Nox protein-derived reactive oxygen species in the  
590 vasculature. *Curr. Opin. Pharmacol.* **2010**, *10*, 122-6.
- 591 37. Sumimoto H., Miyano K.; Takeya R. Molecular composition and regulation of the Nox family  
592 NAD(P)H oxidases. *Biochem. Biophys. Res. Commun.* **2005**, *338*, 677-86.
- 593 38. Drummond G. R., Selemidis S., Griendling K. K.; Sobey C. G. Combating oxidative stress in  
594 vascular disease: NADPH oxidases as therapeutic targets. *Nat. Rev. Drug Discov.* **2011**, *10*, 453-71.
- 595 39. Lim T.-G., Jung S. K., Kim J.-e., Kim Y., Lee H. J., Jang T. S.; Lee K. W. NADPH oxidase is a  
596 novel target of delphinidin for the inhibition of UVB-induced MMP-1 expression in human dermal  
597 fibroblasts. *Exp. Dermatol.* **2013**, *22*, 428-30.

- 598 40. Cimino F., Speciale A., Anwar S., Canali R., Ricciardi E., Virgili F., Trombetta D.; Saija A.  
599 Anthocyanins protect human endothelial cells from mild hyperoxia damage through modulation of  
600 Nrf2 pathway. *Genes Nutr.* **2013**, *8*, 391-9.
- 601 41. Inoue H., Maeda-Yamamoto M., Nesumi A.; Murakami A. Delphinidin-3-O-galactoside  
602 protects mouse hepatocytes from (-)-epigallocatechin-3-gallate-induced cytotoxicity via up-  
603 regulation of heme oxygenase-1 and heat shock protein 70. *Nutr. Res.* **2012**, *32*, 357-64.
- 604 42. Liang C., Xue Z., Cang J., Wang H.; Li P. Dimethyl sulfoxide induces heme oxygenase-1  
605 expression via JNKs and Nrf2 pathways in human umbilical vein endothelial cells. *Mol. Cell*  
606 *Biochem.* **2011**, *355*, 109-15.
- 607 43. Baudin B., Bruneel A., Bosselut N.; Vaubourdolle M. A protocol for isolation and culture of  
608 human umbilical vein endothelial cells. *Nat. Protoc.* **2007**, *2*, 481-5.
- 609 44. Edirisinghe I., Banaszewski K., Cappozzo J., McCarthy D.; Burton-Freeman B. M. Effect of  
610 Black Currant Anthocyanins on the Activation of Endothelial Nitric Oxide Synthase (eNOS) in  
611 Vitro in Human Endothelial Cells. *J Agric. Food Chem.* **2011**, *59*, 8616-24.
- 612 45. Alvarez E., Rodino-Janeiro B. K., Uceda-Somoza R.; Gonzalez-Juanatey J. R. Pravastatin  
613 counteracts angiotensin II-induced upregulation and activation of NADPH oxidase at plasma  
614 membrane of human endothelial cells. *J Cardiovasc. Pharmacol.* **2010**, *55*, 203-12.

615

616

## FIGURE CAPTIONS

617

618

619 **Figure 1.** Chemical structures of the anthocyanin cyanidin-3-glucoside (A), its B-ring degradation  
620 product protocatechuic acid (B), and the mono-*O*-methylated metabolite of protocatechuic acid,  
621 vanillic acid (C). COMT, catechol-*O*-methyltransferase.

622

623 **Figure 2.** Modulation of endothelial eNOS expression (as quantified by ELISA of cell lysates)  
624 following 24 h incubation of HUVECs with vehicle control [0.05% DMSO in supplemented culture  
625 medium] (VC), or 0.1-10  $\mu$ M of cyanidin-3-glucoside (A), protocatechuic acid (B), and vanillic  
626 acid (C). Data are graphed as mean eNOS protein as percentage of vehicle control (designated as  
627 100% and marked by dashed line); mean  $\pm$  SD (n=3). \*Significant difference versus vehicle control  
628 (p < 0.05).

629

630 **Figure 3.** Modulation of angiotensin II (Ang II)-stimulated HUVEC endothelial superoxide  
631 production by 0.1-10  $\mu$ M cyanidin-3-glucoside (A), protocatechuic acid (B), or vanillic acid (C).  
632 Superoxide production was quantified by reduction of extracellular ferricytochrome c. Data are  
633 graphed as SOD-corrected mean absorbance (OD) ratio (550 nm/620 nm) as percentage of Ang II  
634 control (designated as 100% and marked by dashed line); mean  $\pm$  SD (n=3). \*Significant difference  
635 versus Ang II-stimulated control (p < 0.05).

636

637 **Figure 4.** Modulation of HUVEC NOX4 (A) or p22<sup>phox</sup> (B) mRNA levels following 4 h incubation  
638 with 0.1  $\mu$ M angiotensin II control (Ang II), or Ang II with 0.1  $\mu$ M, 1  $\mu$ M or 10  $\mu$ M vanillic acid,  
639 presented as fold change versus unstimulated cells (basal; designated as 1 and marked by dashed  
640 line). Relative quantification was performed by RT-qPCR using the comparative C<sub>t</sub> method,  
641 incorporating the geometric mean of reference genes UBE4A and VIPAS39 as the normalisation

642 factor. Data are graphed as mean  $\pm$  SD (n=3). \*Significant difference versus Ang II-stimulated  
643 control ( $p < 0.05$ ).

644

645 **Figure 5.** Expression of NOX4 protein in cell lysates from unstimulated HUVECs (basal) and  
646 following 6 h incubation with 0.1  $\mu$ M angiotensin II (Ang II), or Ang II with 0.1  $\mu$ M, 1  $\mu$ M or 10  
647  $\mu$ M vanillic acid (VA). Glyceraldehyde-3-phosphate dehydrogenase (GAPDH) was utilised as a  
648 loading control for immunoblotting of cell lysates. Graphs show fold increase in NOX4 expression  
649 relative to basal (designated as 1 and marked by dashed line), after quantification by densitometry  
650 and normalisation to loading control (mean  $\pm$  SD, n=5).

651

652 **Figure 6.** Expression of p47<sup>phox</sup> protein in HUVEC (A) or HCAEC (B) lysates from unstimulated  
653 cells (basal) and following 5 h incubation with 20ng/ml TNF- $\alpha$ , or TNF- $\alpha$  with 0.1  $\mu$ M, 1  $\mu$ M or 10  
654  $\mu$ M vanillic acid. Glyceraldehyde-3-phosphate dehydrogenase (GAPDH) was utilised as a loading  
655 control for immunoblotting of cell lysates. Graphs show fold increase in p47<sup>phox</sup> expression relative  
656 to basal (designated as 1 and marked by dashed line), after quantification by densitometry and  
657 normalisation to loading control. Data are graphed as mean  $\pm$  SD (n=5 for HUVEC and n=4 for  
658 HCAEC).

659

660 **Figure 7.** Modulation of HUVEC HO-1 mRNA levels following 6 h incubation with vehicle control  
661 (VC, 0.005% DMSO), 10 ng/ml phorbol 12-myristate 13-acetate (PMA), or 0.1  $\mu$ M, 1  $\mu$ M or 10  
662  $\mu$ M vanillic acid, presented as fold change versus untreated (basal) cells (designated as 1 and  
663 marked by dashed line). Relative quantification was performed by RT-qPCR using the comparative  
664 C<sub>t</sub> method, incorporating the geometric mean of human reference genes TYW1 and PPIA as the  
665 normalisation factor. Data are graphed as mean  $\pm$  SD (n=3). \*Significant difference versus vehicle  
666 control (\* $p < 0.01$ ).

667

668 **Figure 8.** Expression of HO-1 protein in HUVEC (A) or HCAEC (B) lysates from untreated cells  
669 (basal) and following 6 h incubation with 10 ng/ml phorbol 12-myristate 13-acetate (PMA), vehicle  
670 control (VC, 0.005% DMSO; HUVEC only) or 0.1  $\mu$ M, 1  $\mu$ M or 10  $\mu$ M vanillic acid.  
671 Glyceraldehyde-3-phosphate dehydrogenase (GAPDH) was utilised as a loading control for  
672 immunoblotting of cell lysates. Graphs show fold increase in HO-1 expression relative to basal  
673 (designated as 1 and marked by dashed line), after quantification by densitometry and normalisation  
674 to loading control. Data are graphed as mean  $\pm$  SD (n=4).  
675

Figure 1

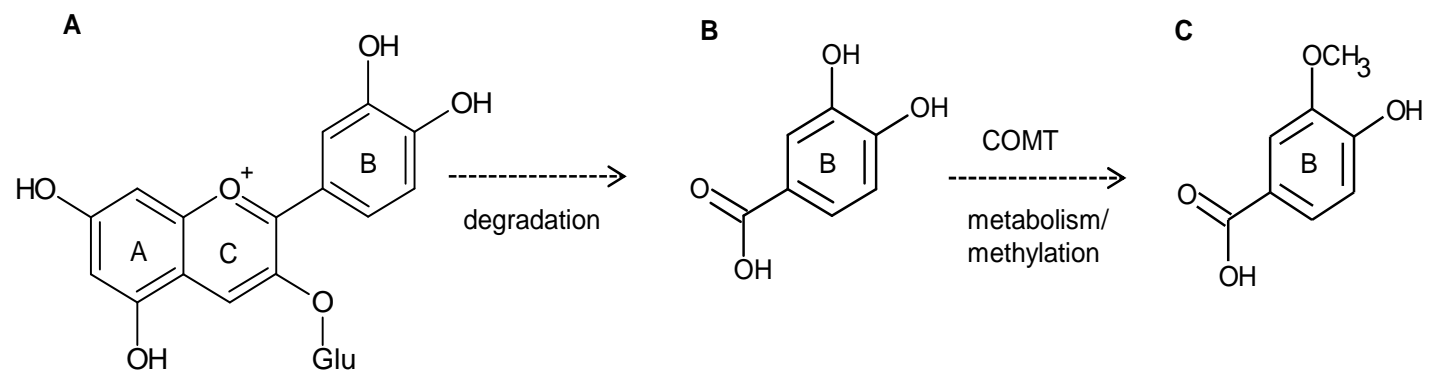


Figure 2

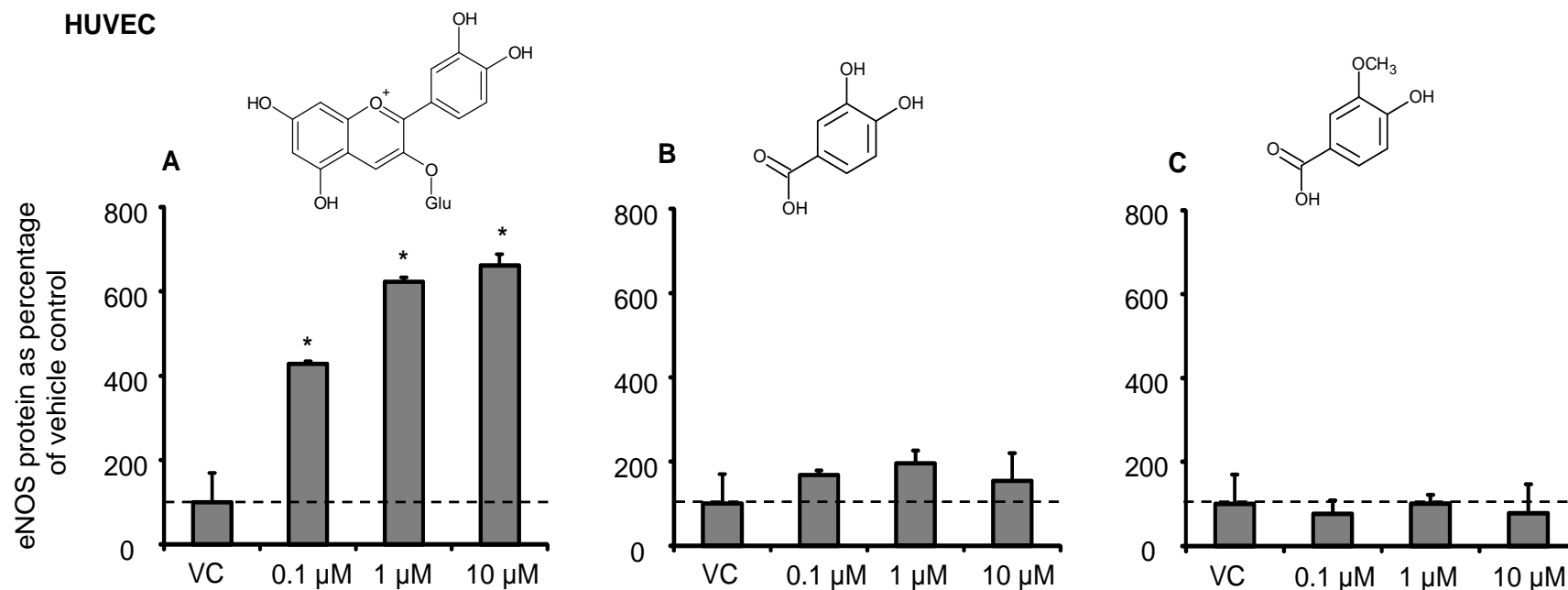


Figure 3

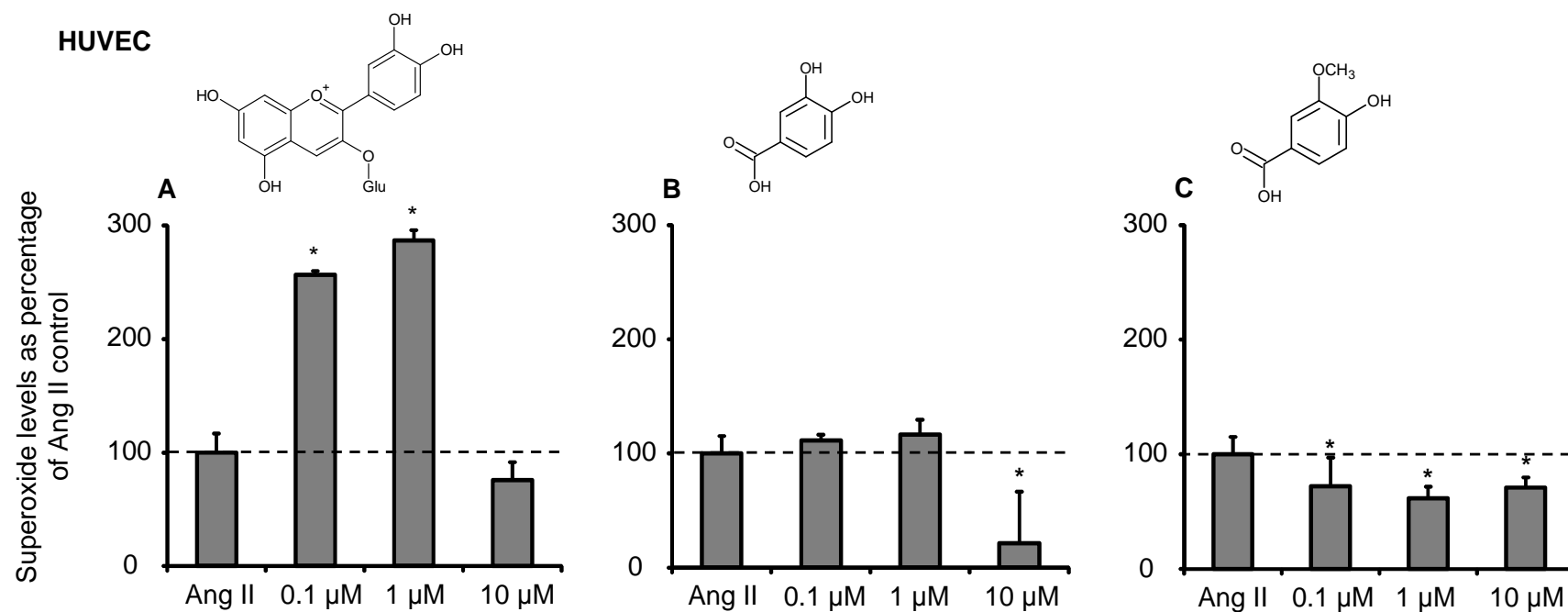


Figure 4

HUVEC

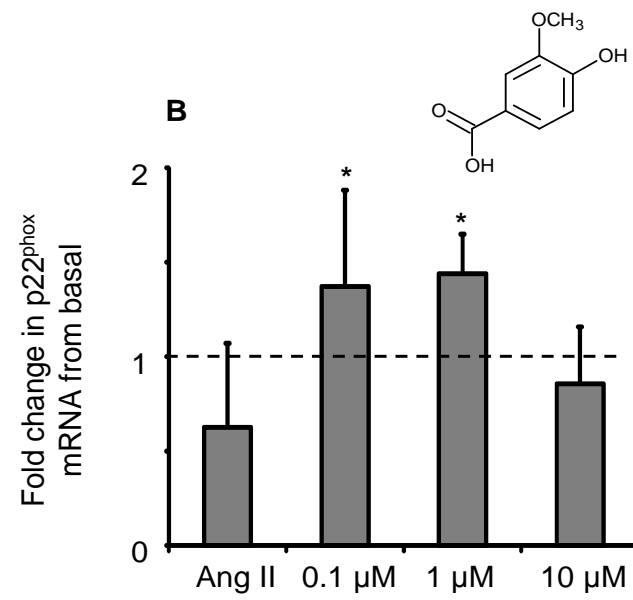
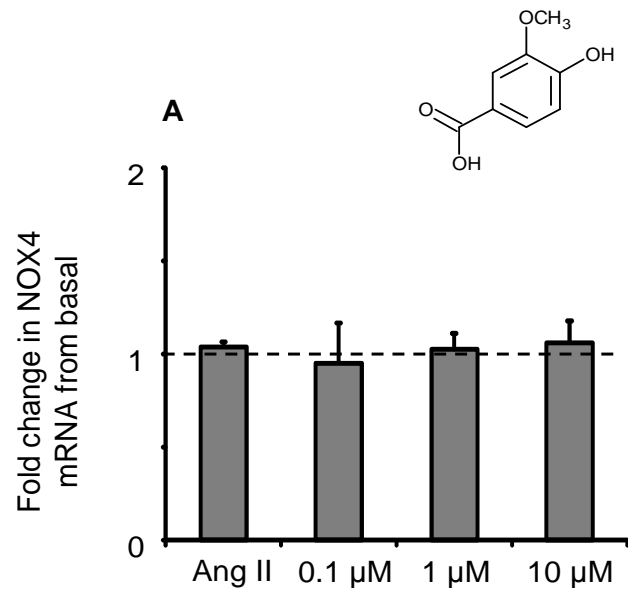


Figure 5

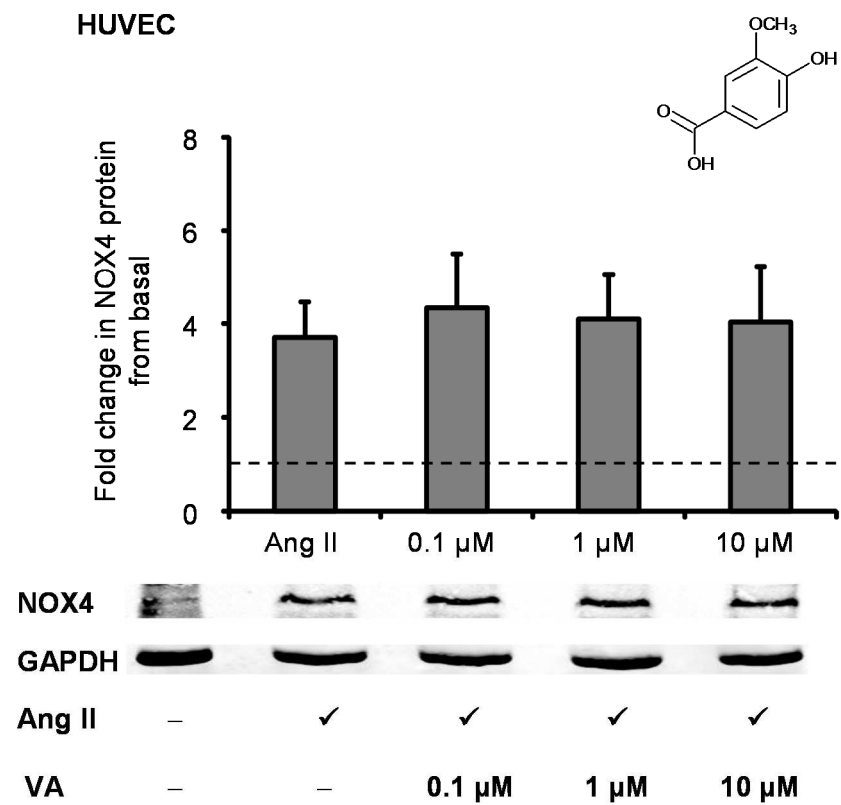


Figure 6

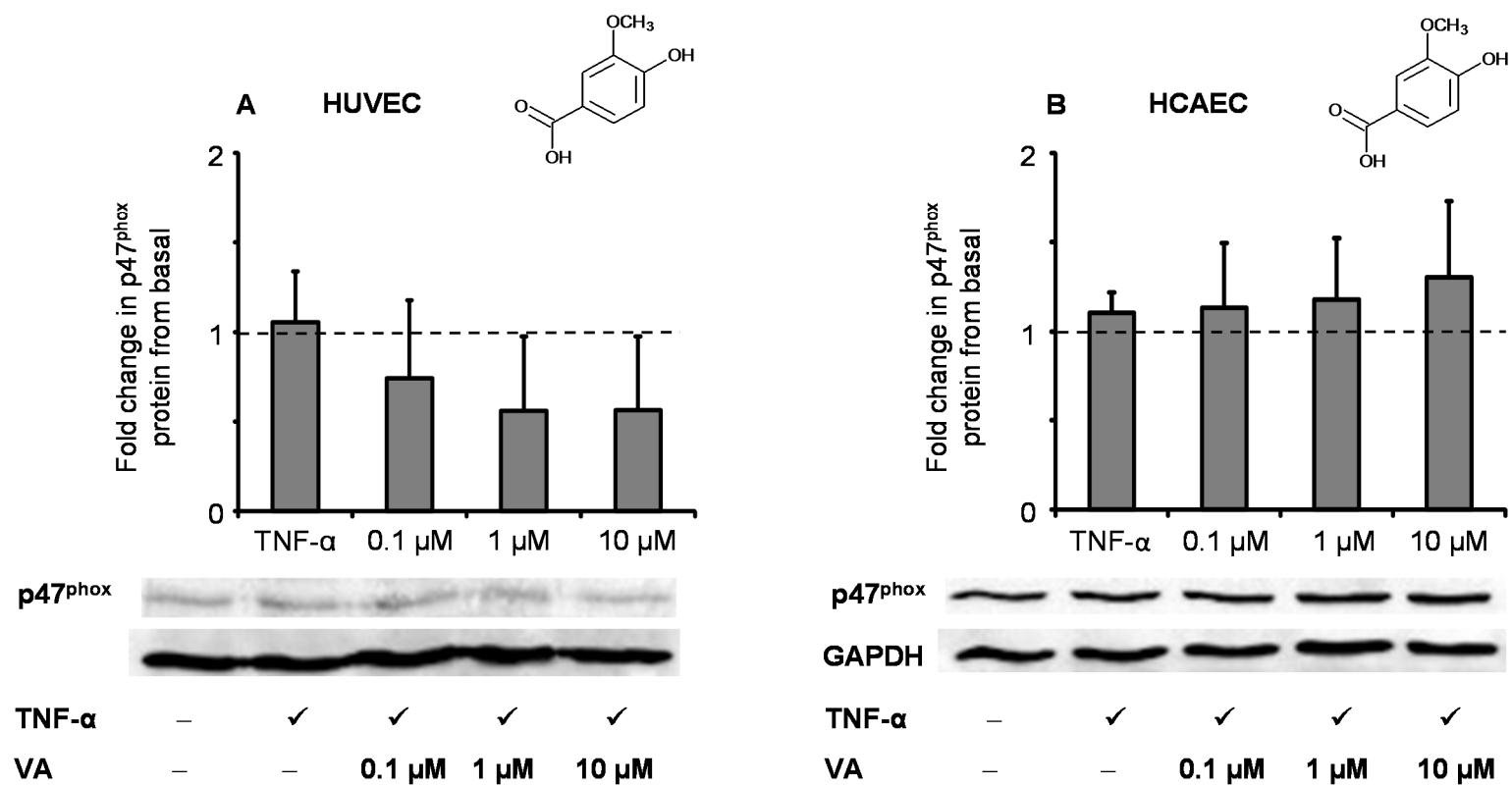


Figure 7

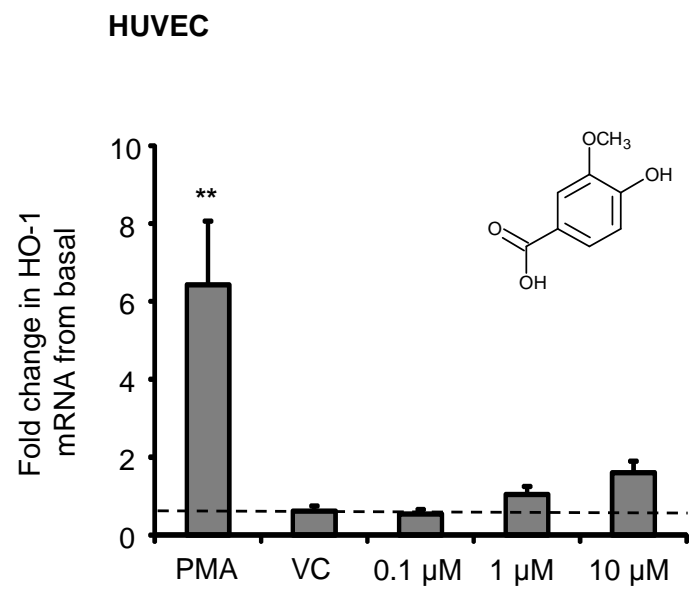


Figure 8

